

A mathematical model of drying processes

PEISHI CHEN and DAVID C. T. PEI

Department of Chemical Engineering, University of Waterloo, Ontario, Canada N2L 3G1

(Received 20 April 1987 and in final form 13 June 1988)

Abstract—A drying model is proposed which may be used to describe drying behavior of hygroscopic and non-hygroscopic materials. The constant rate, the first falling rate and the second falling rate periods in drying are addressed separately. The concept of 'bound water conductivity' is introduced. Movement of bound water and its contribution to moisture transfer within hygroscopic materials are discussed. The bound water conductivity is found to be affected by moisture content as well as desorption isotherms of the drying material. The major internal moisture transfer mechanisms are considered to be capillary flow of free water in the wet region and movement of bound water and vapor transfer in the sorption region. The convective heat and mass transfer coefficients are assumed to vary with the surface free water content in the first falling rate period. Three systems with different hygroscopic properties, wool, brick and corn kernels, are chosen to evaluate the validity of this model. The moving finite element method is used to solve the differential equations numerically. The predicted drying curves and the temperature and moisture distributions compare favorably with reported experimental results.

INTRODUCTION

DRYING is one of the most energy-intensive processes in industry. In order to improve process performance and energy utilization, new technologies such as fluidized bed and spouting bed drying, freeze drying, spray drying and dielectrically-assisted convective drying have been applied. Therefore, it was desired to develop an accurate mathematical model of sufficient generality to evaluate relative performance of various drying processes in materials having diverse moisture transport properties.

Several theoretical models have been proposed in the study of drying processes [1, 2]. In the classical liquid diffusion model proposed by Sherwood [3, 4], Fick's law is assumed to be valid, and the gradient of liquid content is considered to be the driving force for moisture transfer. However, the agreement between theoretical and experimental moisture content profiles was not satisfactory; as pointed out by Ceaglske and Hougen [5], the term 'liquid diffusion' is constrained and may sometimes be misleading.

King [6] proposed a vapor diffusion model for drying of food materials, assuming that vapor diffusion is the only mechanism of internal moisture transfer, and that the relationship between the sorptive moisture and the partial vapor pressure in the gas phase is described by desorption isotherms. Based on the evaporation-condensation theory proposed by Henry [7], Harmathy [8] developed a model of simultaneous heat and mass transfer during the pendular state of liquid within porous materials. The equations derived are the same as those of the vapor diffusion model.

In drying of a wet porous material, internal liquid moisture transport is mainly by capillary flow [5, 9, 10]. By considering that moisture can migrate simultaneously in the forms of capillary flow and vapor

diffusion, Krischer and Kast [11] proposed a multi-mechanism model. A model was proposed for hygroscopic materials based on Krischer and Kast's analysis in ref. [12], assuming that, for moisture content greater than the maximum sorptive value, the vapor pressure in the gas phase is equal to the saturated value. The Clausius-Clapeyron equation is used for coupling phase equilibrium. In the sorption region, the desorption isotherms obtained from experiments are used to determine the vapor pressure. However, in both models, the following factors were not considered:

- (1) the influence of moisture content on each mechanism;
- (2) the importance of movement of bound water and desorption isotherm in drying hygroscopic materials.

Luikov [13] developed a uniquely different approach to the representation of the simultaneous heat and moisture transfer in drying processes, which is based on irreversible thermodynamics. A difficulty with this formulation is that a number of transfer mechanisms are lumped together, masking the individual differences between mechanisms, and the dependence of each on different controlling variables.

In order to describe the simultaneous heat and moisture transfer during the falling rate period in drying of capillary-porous bodies, Luikov [14] proposed a two-zone model. This model assumes the existence of a receding evaporation front which separates the material into a moist zone and an evaporation zone, each with different moisture transfer coefficients. Based on Luikov's two-zone model and the assumption that, in the evaporation zone, moisture transfer is in vapor form only, some solutions for a porous half space system were obtained by Mikhailov [15].

NOMENCLATURE

A	area [m^2]	T	temperature [K]
a, b, c	constants, equation (1) [—]	U	moisture content [kg kg(solid)^{-1}]
c_p	specific heat capacity [$\text{J kg}^{-1} \text{K}^{-1}$]	v	fluid velocity [m s^{-1}].
D_b	bound water conductivity [$\text{m}^2 \text{s}^{-1}$]	Greek symbols	
D_L	capillary conductivity [$\text{m}^2 \text{s}^{-1}$]	α	thermal diffusivity [$\text{m}^2 \text{s}^{-1}$]
D_v	vapor diffusion coefficient [$\text{m}^2 \text{s}^{-1}$]	β	parameter, equation (12)
D'_v	vapor transfer coefficient, equation (20) [$\text{m}^2 \text{s}^{-1}$]	γ	pore volume density function [m^{-1}]
E_d	activation energy of movement of bound water [$\text{kJ kg}^{-1} \text{mol}^{-1}$]	ε	voidage, porosity [—]
h	convective heat transfer coefficient [$\text{W m}^{-2} \text{K}^{-1}$]	η_m, η_h	parameters, equations (22) and (23) [—]
h_m	convective mass transfer coefficient [m s^{-1}]	θ_1, θ_2	parameters, equation (21)
Δh_v	heat of evaporation [kJ kg^{-1}]	λ	mean free path of water molecules [m]
J_L	free water flux [$\text{kg m}^{-2} \text{s}^{-1}$]	μ	viscosity [$\text{kg m}^{-1} \text{s}^{-1}$]
k	thermal conductivity [$\text{W m}^{-1} \text{K}^{-1}$]	ρ	density [kg m^{-3}]
K	permeability [m^2]	σ	surface tension [N m^{-1}]
K_0	single phase permeability of porous material [m^2]	τ	tortuosity factor of capillary paths [—]
K_r	relative permeability [—]	ψ	relative humidity [—].
m	ratio of the diffusion coefficients of air and water vapor [—]	Subscripts	
m_{ev}	evaporation rate [$\text{kg m}^{-3} \text{s}^{-1}$]	0	initial
M	molecular weight	1	wet region
Nu	Nusselt number, hR/k_a [—]	2	sorption region
P	pressure [N m^{-2}]	a	air
P_c	capillary pressure, $P_g - P_L$ [N m^{-2}]	b	bound water
P_v	vapor pressure [N m^{-2}]	c	capillary, critical
Pr	Prandtl number, $k_a c_{pa} / \mu_a$ [—]	eq	equilibrium
q	heat source [W m^{-3}]	g	gas phase
r, R	radius [m]	h	heat
R	gas constant [$\text{kJ kg}^{-1} \text{mol}^{-1} \text{K}^{-1}$]	ir	irreducible
Re	Reynolds number, $Rv_a \rho_a / \mu_a$ [—]	L	liquid moisture, free water
S	pore saturation [—]	m	mass
$S(t)$	position of receding evaporation front [m]	ms	maximum sorptive
Sh	Sherwood number, $h_m R / D_v$ [—]	s	water saturated
t	time [s]	v	vapor
		w	water, wet bulb.
		Superscript	
		*	vapor saturated.

Szentgyorgyi and Molnar [16] proposed a two-zone model based on the diffusion model. By assuming that a constant moisture content is equal to that in sorption equilibrium with the drying medium in the dry zone, a solution was obtained. A fairly satisfactory approximation of temperature distribution was predicted, as compared with the experimental results.

Most of the models described above have not been able to predict drying rates and the distribution of temperature and moisture content for both hygroscopic and non-hygroscopic materials over a wide range of boundary conditions and drying regimes. This is because, the moisture transport in materials is caused by a variety of mechanisms [1, 17–20], each of which is prevalent under different conditions. The local moisture content, temperature and the hygro-

scopic properties influence the contribution of each mechanism and consequently affect the drying rate. In general, moisture transport in the dry zone is not simple, and the moisture content in each zone is not constant. Furthermore, for porous materials, the convective mass transfer coefficient varies with the surface moisture content [21, 22].

The convective heat and mass transfer coefficients at the surface are important parameters in drying processes; they are functions of velocity and physical properties of the drying medium [23], and in general, can be expressed in the form

$$Nu = a Re^b Pr^c \quad (1)$$

$$Sh = a' Re^{b'} Sc^{c'} \quad (2)$$

In the present study, a mathematical model for drying processes is developed, which considers all the major internal moisture transfer mechanisms and the properties of the material to be dried, including whether it is hygroscopic or non-hygroscopic. The convective heat and mass transfer coefficients are assumed to vary with the surface moisture content. A moving finite-element method is used to solve the differential equations numerically.

The physical configuration for the present model is shown in Fig. 1. When a porous material is exposed to a convective surface condition, three main mechanisms of internal moisture transfer are assumed to prevail, capillary flow of free water, movement of

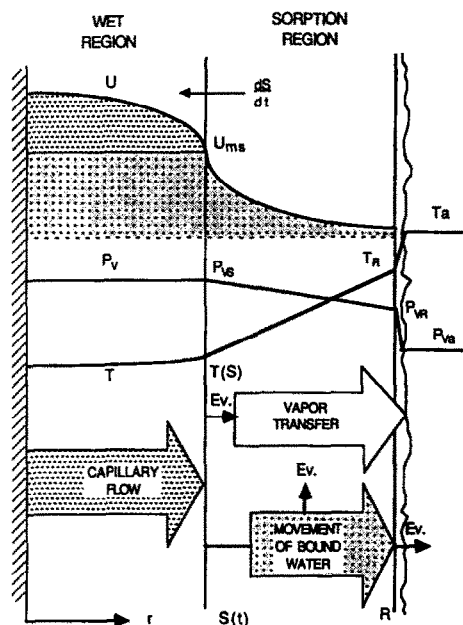


FIG. 1. Drying model.

Regardless of the rate of internal moisture transfer, so long as the free water content at the surface is less than the critical, the surface will form discontinuous wet patches. Thus, the mass transfer coefficient decreases with the surface free water content and the first falling rate period starts. In the first falling rate period, a new energy balance will be reached at the surface, accompanied by a slowly rising surface temperature. Free water still exists at the surface, the 'dry' patches still contain bound water, and the vapor pressure at the surface is determined by the Clausius-Clapeyron equation.

When the surface moisture content reaches its maximum sorptive value, no free water exists. The surface temperature will rise rapidly, signaling the start of the second falling rate period, during which a receding evaporation front often appears, dividing the system into two regions, the wet region and the sorption region. Inside the evaporation front, the material is wet, i.e. the voids contain free water and the main mechanism of moisture transfer is capillary flow. Outside the front, no free water exists. All water is in the sorptive or bound water state and the main mechanisms of moisture transfer are movement of bound water and vapor transfer. Evaporation takes place at the front as well as in the whole sorption region, while vapor flows through the sorption region to the surface.

With the above definitions of the constant rate, first falling rate and second falling rate periods, the characteristics of most drying processes can be described mathematically.

Since the internal moisture transport mechanisms, the desorption isotherms, and the convective heat and mass transfer coefficients are all important factors in the model, they will be discussed in turn.

Capillary flow of free water

In porous materials, voids provide capillary paths for free water to flow. The driving force for capillary flow is tension gradient or pressure gradient. The pertinent expression [9, 10] for capillary flow of free water is given by

$$J_L = -\rho_w \frac{K_L}{\mu} (\nabla P_g - \nabla P_c - \rho_w \mathbf{g}). \quad (3)$$

For most drying processes, we can assume that:

- (1) the material is macroscopically homogeneous;
- (2) the flow in the capillary paths is laminar;
- (3) there is no significant temperature gradient;
- (4) the effect of the gas phase pressure and gravity force are negligible.

Thus, equation (3) can be simplified as

$$J_L = \rho_w \frac{K_L}{\mu} \nabla P_c = \rho_w \frac{K_r K_0}{\mu} \nabla P_c. \quad (4)$$

As pointed out by Miller and Miller [26], for homogeneous media and negligible gravity forces, tension is proportional to moisture content. It appears that Krischer and Kast's equation for liquid flow [11] may be valid

$$J_L = -\rho_0 D_L \nabla U \quad (5)$$

where ρ_0 is the bulk density of dry material.

Since the permeability K_L depends on the pore structure of the material and the interaction between water and the solid skeleton, it is difficult to find a theoretical form to relate K_L and the capillary conductivity D_L . However, the velocity of flow in capil-

aries may be assumed to follow the Hagen-Poiseuille law [23]

$$v = \frac{r^2}{8\mu\tau} \nabla P_c. \quad (6)$$

The total mass flow rate of free water can then be expressed in terms of the local velocity and corresponding capillary radius, r_c , which is defined as the radius of the largest capillary in which free water exists, i.e.

$$J_L = \frac{1}{A} \int \rho_w \frac{r^2}{8\mu\tau} \nabla P_c dA_c = \int_{r_{\min}}^{r_c} \rho_w \frac{r^2}{8\mu\tau} \nabla P_c \gamma(r) dr \quad (7)$$

where $\gamma(r)$ is the pore volume density function, defined as

$$\gamma(r) = \frac{\rho_0}{\rho_w} \frac{\Delta U}{\Delta r} \bigg|_r = \varepsilon \frac{\Delta S}{\Delta r} \bigg|_r.$$

The relationship between the pore saturation and the pore density function is

$$S = \frac{\int_{r_{\min}}^{r_c} \gamma(r) dr}{\int_{r_{\min}}^{r_{\max}} \gamma(r) dr} = \frac{1}{\varepsilon} \frac{\int_{r_{\min}}^{r_c} \gamma(r) dr}{\int_{r_{\min}}^{r_{\max}} \gamma(r) dr} \quad (8)$$

where r_{\max} is the overall largest capillary in the porous material. Comparing equations (4) and (5) with equation (7), K_L may be expressed as

$$K_L = K_r K_0 = \int_{r_{\min}}^{r_c} \frac{r^2}{8\tau} \gamma(r) dr \quad (9)$$

and the capillary conductivity D_L may be expressed as

$$D_L = -\frac{K_L}{\mu} \frac{\rho_w \nabla P_c}{\rho_0 \nabla U} = \frac{2}{r_c^2 \gamma(r_c)} \frac{\sigma}{\mu} K_L. \quad (10)$$

The pore volume density function can be obtained from the relationship between capillary pressure and pore saturation of a porous medium. Solving equations (8) and (9) using the correlation of pore volume density obtained from the experimental results of Chatzis [27], a relationship between pore saturation and relative permeability can be obtained which is very close to the empirical correlation

$$K_r = \left(\frac{S - S_{ir}}{1 - S_{ir}} \right)^3. \quad (11)$$

Therefore, equation (11) can be used to predict the relative permeability, K_r . For water, σ/μ is a linear function of temperature [17], which can be expressed as

$$\frac{\sigma}{\mu} = 1.604T - 394.3 (\text{m s}^{-1}). \quad (12)$$

The value of $r_c^2 \gamma(r_c)$ in equation (10) might be constant

or a function of free water content. Consequently, the following form is obtained to predict the capillary conductivity of free water for non-hygroscopic materials:

$$D_L = (1.604T - 394.3)\beta K_0 \left(\frac{S - S_{ir}}{1 - S_{ir}} \right)^3 \quad (13)$$

and similarly, for hygroscopic materials

$$D_L = (1.604T - 394.3)\beta K_0 \left(\frac{U - U_{ms}}{U_s - U_{ms}} \right)^3.$$

Movement of bound water

Movement of bound water, sometimes known as 'liquid moisture transfer near dryness' or 'sorption diffusion', has been studied by a number of investigators [17–20, 24, 28]. It has been shown that liquid moisture transfer still exists in the sorption region and is a strong function of free water content. Whitaker [20, 29] studied gas phase convective transport in the 'dry' region which contains irreducible water and concluded that there could be a liquid moisture flux in that region. Bramhall [28] proposed a 'sorption diffusion' model for the wood drying process which assumed that, when the adsorbed water molecules receive enough energy to break the sorptive bonds, they may leave and migrate until captured by other sites. The energy is then received by other molecules and the process is repeated. He also tried to show that the activation energy of 'sorption diffusion' is the same as the evaporation heat of water.

Movement of bound water however cannot be simply defined as a diffusion process, which often creates confusion in the analysis of liquid moisture transfer in drying processes. Moreover, the bound water conductivity measured is strongly influenced by moisture content. Therefore, movement of bound water may rather be due to flow along very fine capillaries or through cellular membranes.

In the present study, for moisture transfer in the sorption region, the following assumptions are made:

(1) bound water exists in any hygroscopic porous material; for food products, the bound water refers to the cellular water [17, 19, 24], and for granular porous material, it refers to the water in the 'dead ends', or very fine capillaries;

(2) liquid transfer in the sorption region is defined as movement of bound water, as shown in Fig. 2; for food products the bound water moves through the semi-permeable membranes along the array of the cellular structure, and for granular porous materials the bound water moves along very fine capillaries;

(3) movement of bound water may have the characteristics of capillary flow, with the driving force being gas phase pressure or vapor pressure gradient;

(4) the bound water conductivity is a strong function of moisture content.

At room temperature, the bound water con-

ductivity depends on the microscopic structure of the material and is of the order of $10^{-9} \text{ m}^2 \text{ s}^{-1}$ [18, 20]. Therefore, in the wet region, it can be neglected compared with the capillary conductivity of free water. However, in the sorption region, both movement of bound water and vapor transfer play important roles in moisture transfer. The transport equation for bound water may be expressed as

$$J_b = -\rho_w \frac{K_b}{\mu} \nabla P = -\rho_w \frac{K'_b}{\mu} \nabla P_v. \quad (14)$$

Since the bound water in the sorption region is in equilibrium with vapor in the gas phase, equation (14) may be written as

$$J_b = -\rho_w \frac{K'_b}{\mu} P_v^* \frac{\partial \psi}{\partial U} \nabla U = -\rho_0 D_b \nabla U \quad (15)$$

where D_b is an Arrhenius-type function of temperature [17, 30]. Thus the bound water conductivity may be written as

$$D_b = D_{b0} \left(\frac{U_b - U_{eq}}{U_{ms} - U_{eq}} \right)^3 \exp \left(-\frac{E_d}{RT} \right) \quad (16)$$

where E_d is defined as the activation energy of movement of bound water. Experimental data in the literature [28, 30] show that the activation energy of bound water movement is different from the vaporization heat of free water because the sorption characteristics of the material influence the movement of bound water. Recently, Okazaki and co-workers [31, 32] studied moisture transfer mechanisms in sorptive porous materials by including the effect of condensate flow in fine capillaries, which may also be regarded as bound water. It is hard to tell whether the water in fine capillaries in a porous material comes from condensation or from connected fine capillaries, but it is clear that movement of bound water plays an important role in moisture transfer in the sorption region.

Vapor flow

During a drying process, water vapor flows through the voids of a porous material by convection and diffusion. The equations for vapor flow and airflow may be written as

$$J_v = \frac{P_v M_w}{RT} \frac{K_g}{\mu_g} \nabla P + \frac{D_v M_w}{RT} \nabla P_v \quad (17)$$

$$J_a = \frac{(P - P_v) M_a}{RT} \frac{K_g}{\mu_g} \nabla P + \frac{m D_v M_a}{RT} \nabla (P - P_v) \quad (18)$$

where m is the ratio of air and vapor diffusion coefficients. Two kinds of diffusion may be important in drying processes, molecular diffusion and Knudsen diffusion. When the capillary size is large in comparison with the mean molecular free path of water vapor, λ , molecular diffusion prevails, and

$$D_v = \frac{\epsilon_g}{\tau} D_{va}.$$

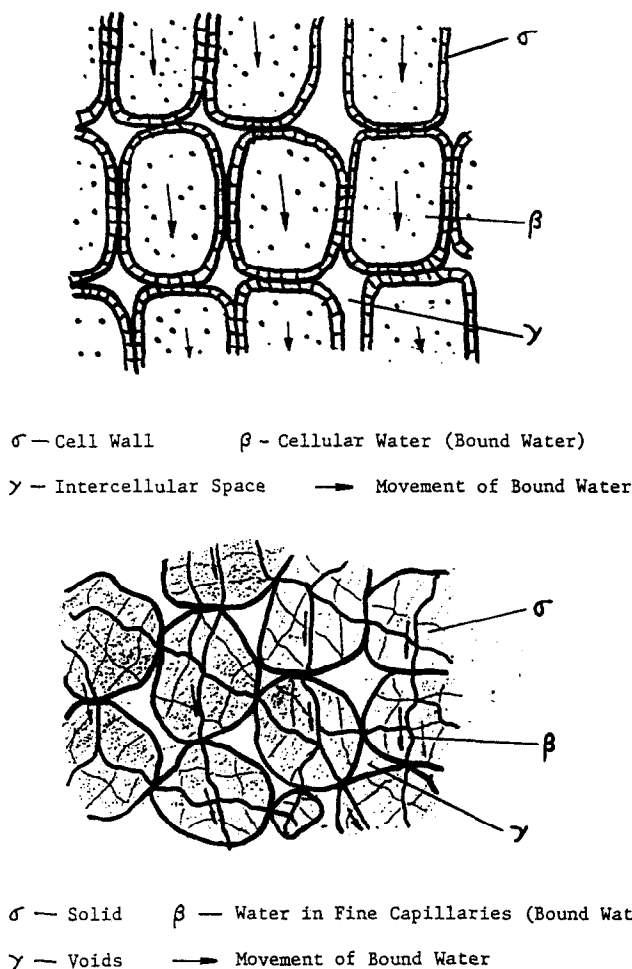


FIG. 2. Movement of bound water.

When the capillary size is equal to or smaller than λ , Knudsen diffusion predominates, and

$$D_v = \frac{\varepsilon_g}{\tau} D_K.$$

By assuming the airflow is negligible, the approximate relationship between gas phase pressure drop and vapor pressure drop can be obtained

$$\frac{\Delta P_v}{\Delta P} = 1 + \frac{K_g}{mD_v\mu_g} (P - P_v). \quad (19)$$

Substituting equation (19) into equation (17)

$$J_v = \frac{D_v M_w}{RT} \left(1 + \frac{\frac{K_g}{\mu_g} P_v}{D_v + \frac{K_g}{m\mu_g} (P - P_v)} \right) \nabla P_v = \frac{D_v' M_w}{RT} \nabla P_v. \quad (20)$$

In most convective drying processes, the temperature gradient in the wet region is small and vapor flow is much less than flow of free water [33]. In the

sorption region, if the local temperature is low, i.e. $P_v \ll P$, the gas phase pressure gradient is small and the contribution of convection to the vapor transfer is small. However, if the temperature approaches the boiling temperature of water, the contribution of convection to vapor transfer becomes significant.

Sorption equilibrium

The interaction between bound water and solid material can be expressed by a sorption equilibrium curve, which shows the relationship between the amount of adsorbed or bound water and relative humidity at a certain temperature. In drying processes, desorption isotherms are often used, as shown in Fig. 3.

In region A, water is more 'tightly' bound to solid and in region B water is more 'loosely' bound. The higher the curve, the stronger the water-solid interaction, the more the bound water in solid.

Several correlations for desorption isotherms have been proposed. The most applicable to food products are the modified Henderson equation [34], and Chung and Pfost's equation [35]. In the present study, the modified Henderson equation is used

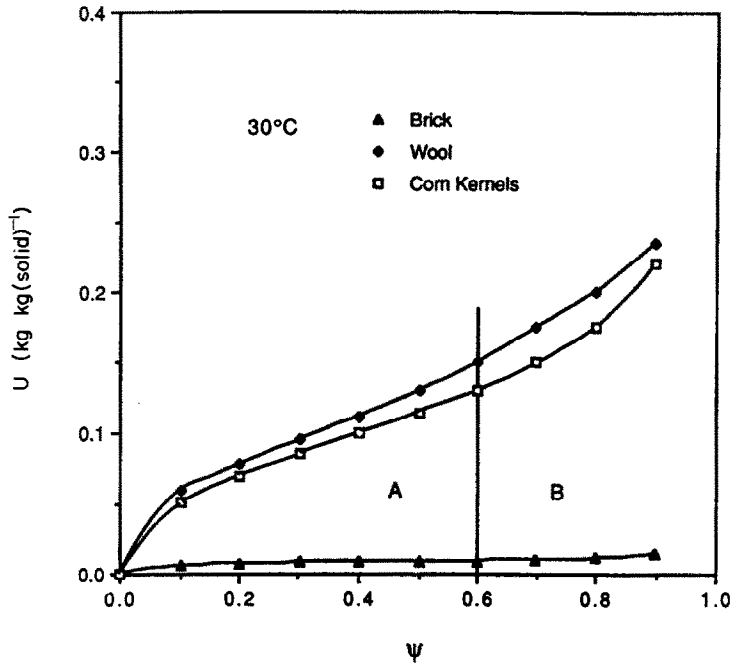


FIG. 3. Desorption isotherms.

$$\psi = \frac{P_v}{P_v^*} = 1 - \exp(-\theta_1 U_b^{\theta_2}) \quad (21) \quad h = h_0 \left(\eta_h + (1 - \eta_h) \frac{U(R) - U_{ms}}{U_c - U_{ms}} \right)$$

where parameters θ_1 and θ_2 are functions of the local temperature.

Convective heat and mass transfer coefficients

As discussed earlier, the convective mass transfer coefficient varies with the fractional wet area at the surface. If the free water content at the surface is greater than about 30% of the saturated free water content, the surface water layer remains continuous, and the drying rate remains constant. For lower free water contents, the continuous film layer breaks into discontinuous wet patches, the mass transfer coefficient decreases, and the drying rate falls. For high intensity drying, the evaporation rate at the surface will be greater than the internal liquid flow required to maintain a continuous surface layer; in this case, the value of the critical moisture content increases, and the continuous film layer becomes discontinuous soon after the drying process starts. Consequently, no obvious constant rate period will be observed [22].

According to the experimental results of Nissan and co-workers [36, 37], it appears that the convective heat transfer coefficient also decreases in the first falling rate period. In the present study, the convective heat transfer coefficient is also considered as a function of the free water content at the surface, and the convective heat and mass transfer coefficients are simply assumed to vary linearly with the free water content in the first falling rate period

$$(U_{ms} < U(R) < U_c) \quad (22)$$

$$h_m = h_{m0} \left(\eta_m + (1 - \eta_m) \frac{U(R) - U_{ms}}{U_c - U_{ms}} \right) \quad (U_{ms} < U(R) < U_c) \quad (23)$$

where η_h and η_m are constants for a given material, their values must be determined by experiment.

MATHEMATICAL FORMULATION

In the present drying model, the wet region ($0 < r < S(t)$) and the sorption region ($S(t) < r < R$) are considered respectively in mathematical formulation.

Wet region

In the wet region, the main mechanism of moisture transfer is capillary flow of free water. The driving force for capillary flow is the capillary pressure gradient. The very small amount of water evaporated in the wet region is also considered. Consequently, the liquid moisture transfer equation can be obtained from the mass balance in the liquid phase

$$\rho_0 \frac{\partial U_1}{\partial t} = \rho_0 \nabla (D_L \nabla U_1) - m_{ev} \quad (24)$$

where m_{ev} denotes the evaporation rate in the wet

region. Accordingly, the vapor transfer equation can be written as

$$\frac{\partial(\epsilon_g \rho_v)}{\partial t} = \nabla \left(\frac{D'_{v1} M_w}{RT} \nabla P_v \right) + m_{ev}. \quad (25)$$

The left-hand side of the equation may be neglected. The heat transfer equation can also be written from energy conservation considerations, and the convective term may be neglected

$$(\rho c_p) \frac{\partial T_1}{\partial t} = \nabla(k_1 \nabla T_1) - m_{ev} \Delta h_v + q_1 \\ = \nabla(k_{eff} \nabla T_1) + q_1 \quad (26)$$

$$k_{eff} = k_1 + \frac{D'_{v1} M_w}{RT} \frac{\partial P_v^*}{\partial T} \Delta h_v$$

where q_1 is the heat source term for dielectric heating in the wet region; it may be assumed to be proportional to the moisture content [38]. If there is no soluble substance in the water, the vapor pressure in the wet region can be calculated from the Clausius–Clapeyron equation.

Sorption region

In the sorption region, the main mechanisms of moisture transport are movement of bound water and vapor transfer. From mass and energy conservation, respectively, the moisture and heat transfer equations in the sorption region can be written as

$$\rho_0 \frac{\partial U_2}{\partial t} = \rho_0 \nabla(D_b \nabla U_2) - m_{ev} \quad (27)$$

$$(\rho c_p)_2 \frac{\partial T_2}{\partial t} = \nabla(k_2 \nabla T_2) - m_{ev} \Delta h_v + q_2 \quad (28)$$

where q_2 is the heat source term for dielectric heating in the sorption region. The evaporation term can be obtained from the vapor transfer equation

$$\frac{\partial(\epsilon_g \rho_v)}{\partial t} = \nabla \left(\frac{D'_{v2} M_w}{RT} \nabla P_v \right) + m_{ev}. \quad (29)$$

The left-hand side of the equation may again be neglected. In the sorption region, the desorption isotherm couples the moisture contents in the solid and gas phases. Therefore, the desorption isotherms are the determinants of the moisture distribution in the sorption region. In the present model, the desorption isotherm is correlated by the modified Henderson equation [34], i.e. equation (21).

Boundary conditions

Due to symmetry of the material, the boundary conditions at the center, or $r = 0$, are

$$\frac{\partial U_1}{\partial r} = 0, \quad \frac{\partial T_1}{\partial r} = 0. \quad (30)$$

The boundary conditions at the surface, or $r = R$, are

$$\frac{D'_{v2} M_w}{RT} \frac{\partial P_v}{\partial r} + \rho_0 D_b \frac{\partial U_2}{\partial r} = \frac{h_m M_w}{RT} (P_{va} - P_v) \quad (31)$$

$$k_2 \frac{\partial T_2}{\partial r} = h(T_a - T_2) + \rho_0 D_b \frac{\partial U_2}{\partial r} \Delta h_v. \quad (32)$$

It should be noted that the convective heat transfer coefficients, h and h_m , are functions of velocity and properties of the flowing medium. During the constant rate period, they may be determined by the classical correlations. In the first falling rate period, they are further affected by the free water content at the surface. Equations (22) and (23) may be used to determine the values of h and h_m .

In the second falling rate period, the evaporation front recedes from the surface and divides the material into the wet region and the sorption region. The free moisture content at the receding evaporation front is zero, and the moisture content is thus equal to the maximum sorptive value. The following moving boundary conditions are obtained from the mass and heat balances at the evaporation front, i.e. at $r = S(t)$

$$T_1 = T_2, \quad U_1 = U_2 = U_{ms} \quad (33)$$

$$\rho_0 D_b \frac{\partial U_1}{\partial r} = \rho_0 D_b \frac{\partial U_2}{\partial r} + \frac{D'_{v2} M_w}{RT} \frac{\partial P_v}{\partial r} \quad (34)$$

$$k_{eff} \frac{\partial T_1}{\partial r} = k_2 \frac{\partial T_2}{\partial r} + \frac{D'_{v2} M_w}{RT} \frac{\partial P_v}{\partial r} \Delta h_v \quad (35)$$

where U_{ms} is the maximum sorptive moisture content. Usually, the substantial derivative of moisture content with respect to time is zero, and the moving velocity of the evaporation front can thus be determined by

$$\frac{dS(t)}{dt} = - \frac{\left(\frac{\partial U_1}{\partial t} \right)_s}{\left(\frac{\partial U_1}{\partial r} \right)_s} \cong - \frac{\nabla(D_b \nabla U_1)_s}{\left(\frac{\partial U_1}{\partial r} \right)_s}. \quad (36)$$

These moving boundary equations are the coupling equations for the heat and mass transfer in the two regions.

Model application

When a very wet porous material is dried by a convective medium, three drying rate periods are often observed, the constant rate period, the first falling rate period and the second falling rate period. In the constant rate period and the first falling rate period, the material remains wet, and the model of the wet region only is used. Since evaporation takes place almost entirely at the surface, the drying rate is controlled by the convective heat and mass transfer. If the temperature gradient within the material is negligible, the surface temperature is almost constant and its value is very close to the wet bulb temperature of the flowing air. Therefore, the following relationship determines the surface temperature in the constant rate period:

$$h(T_a - T_w) = \frac{h_m M_w \Delta h_v}{RT} (P_{vw}^* - P_{va}). \quad (37)$$

When the free water content at the surface is less than the critical value (30% of the saturated free water content), the first falling rate period starts, and equations (22) and (23) are used to determine the convective heat and mass transfer coefficients. In this period, the surface temperature rises slowly, and may also be determined by equation (37).

When the free water content at the surface reaches zero, the second falling rate period starts and the two-region model is used. During the second falling rate period, the evaporation front recedes from the surface, and evaporation takes place mainly at the evaporation front as well as in the sorption region. As the amount of water evaporating from the surface decreases quickly, the surface temperature rises much faster than that in the first falling rate period.

Sometimes the initial moisture content of the material is equal to or less than the maximum sorption moisture content and no constant rate period will appear, such as in many grain drying processes. In that case, the model of the sorption region only is used.

Freeze drying process

The freeze drying process with dielectric heating appears to be a promising technique to accelerate the drying rate. Dielectric power is more effective for sublimating and thus overcoming the heat transfer barrier of the dry or sorption region. Some theoretical analysis of microwave heating freeze drying was studied by Ang *et al.* [39] and Ma and Peltre [40].

According to the present study, microwave heating freeze drying is just a special case of the drying problem. The moving boundary in freeze drying is the sublimation front, which separates the system into two regions, the frozen region and the dry or sorption region. Drying takes place at the sublimation front and in the sorption region. In the frozen region, the moisture is in the solid state, therefore the moisture content remains constant.

NUMERICAL SOLUTIONS AND COMPARISON WITH EXPERIMENTAL RESULTS

In order to test the validity of the mathematical model, three materials with different sorption properties were chosen for comparison: wool bobbins, brick slabs and corn kernels. Brick is a non-hygroscopic porous material, while wool and corn kernels are hygroscopic materials with different structures. In most cases, the initial moisture content is equal to or less than the maximum sorption value and according to the present model, no constant rate period will be observed. Furthermore, the desorption isotherms of these materials are documented, which makes it possible to accurately simulate the drying processes.

The finite element method with Galerkin for-

mulation has been well established to solve non-linear transient problems [41, 42]; in the present study, it was used and expanded to solve the drying problem. Elements can be built in finer structure in areas adjacent to the moving boundary to enhance the accuracy.

Drying of wool

Nissan and co-workers [36, 37] performed experiments on the drying of wool bobbins in an air tunnel. The wool, composed of bulk yarn in a hairy felted cloth wound on Bakelite bobbins was dried by a hot air stream parallel to the axis of the cylinder. The wool package had a 15 cm length, 7.36 cm o.d. and 1.58 cm i.d. The drying conditions and the physical properties are listed in Table 1.

The hygroscopic nature of wool has been studied by Walker [43]. The reported data are correlated in the form of equation (21)

$$\psi = \frac{P_v}{P_v^*} = 1 - \exp(-(154.5 - 0.359T)U_2^{(4.51 - 0.0087T)}). \quad (38)$$

Equations (13) and (16) were used to determine the capillary conductivity of free water in the wet region and the bound water conductivity in the sorption region. The heat and mass transfer coefficients in the first falling rate period may be determined by the following equations:

$$h = h_0 \left(0.60 + 0.40 \frac{U(R) - U_{ms}}{U_c - U_{ms}} \right) \quad (39)$$

$$h_m = h_{m0} \left(0.50 + 0.50 \frac{U(R) - U_{ms}}{U_c - U_{ms}} \right). \quad (40)$$

By using the moving finite element method, the numerical solutions of this problem were obtained. Figure 4 shows the variation of moisture content with time. The computed results show that the drying process can be divided into the heating-up period, the constant rate period, the first falling rate period and the second falling rate period. The first falling rate period starts at 60 min, when the free water content at the surface equals 30% of the saturated free water content or $U(R) = U_c$.

When the free water content at the surface equals zero, that is at about 110 min, the second falling rate period starts, and the two-region drying model is used. The predicted moisture and temperature distributions are plotted in Figs. 5 and 6, and compared with the experimental data. As can be seen from Fig. 5, the predicted moisture distribution at 60 min agrees well with the data. However, the predicted moisture distribution at the beginning of the second falling rate period does not. This is because, at the beginning of the second falling rate period, the free water content at the surface is zero, or the surface moisture content is equal to the maximum sorptive value, which is difficult to measure at the real surface. It might only be observed when a thin surface layer is dried and the

Table 1. Physical properties and drying conditions

Properties	Wool	Brick	Corn kernels
ρ_0	283	1450	1236
ϵ	0.76	0.435	0.12
c_p	$1.25+4.18\ U$	$0.75+4.18\ U$	$1.46+3.97\ U$
k	$0.05+0.18\ U$	$0.50+0.58\ U$	$0.07+0.65\ U$
βK_0	4.0×10^{-9}	7.8×10^{-9}	—
D_{b0}	0.062	0.098	0.0001
E_d/R	4830	5200	3900
U_c	1.14	0.09	—
Drying conditions			
$T_a(^{\circ}\text{C})$	78.5	80	71
v_a	5.25	5.0	2.33
ψ	0.03	0.093	0.118
h_0	64.8	75	33
h_{m0}	0.065	0.083	0.026
U_0	2.64	0.168	0.31
$T_0(^{\circ}\text{C})$	18	25	20

moisture content is equal to the maximum sorptive value. The predicted moisture distribution at 130 min agrees well with the measured distribution at the ‘beginning’ of the second falling rate period. In Fig. 6, it can be seen that the predicted temperature distribution agrees well with the experimental data.

Drying of bricks

Przesmycki and Strumillo [44] studied the drying of brick and clay slabs. The brick slab had an area of 20 cm² and a thickness of 5 cm. They also proposed a three-zone model including a wet zone, an evaporation zone and a dry zone. However, there was no information on how the positions of the two moving boundaries were determined and when the first or second falling rate periods were supposed to start.

The drying conditions and the physical properties of brick are listed in Table 1. The data of the desorption isotherm of brick were given by Haertling [45], which may be correlated as

$$U_2 = 0.0105\psi^{0.2} + 0.0125 \exp(20\psi - 20). \tag{41}$$

Since the maximum sorption moisture content is very low (about 0.015), brick is usually regarded as a non-hygroscopic material.

The convective heat and mass transfer coefficients in the first falling rate period may have the following relationship with the free water content at the surface :

$$h = h_0 \left(0.80 + 0.20 \frac{U(R) - U_{ms}}{U_c - U_{ms}} \right) \tag{42}$$

$$h_m = h_{m0} \left(0.10 + 0.90 \frac{U(R) - U_{ms}}{U_c - U_{ms}} \right). \tag{43}$$

The numerical solutions for brick slabs are shown

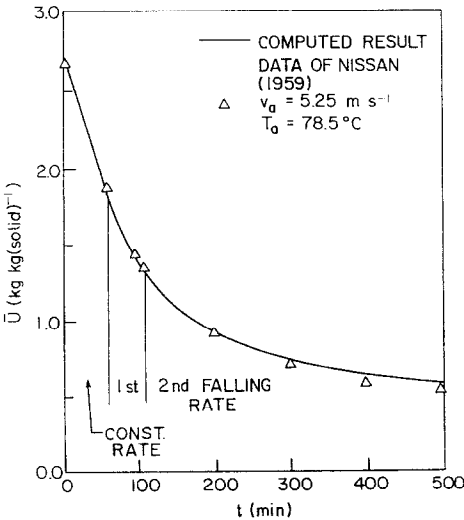


FIG. 4. Drying curve of wool.

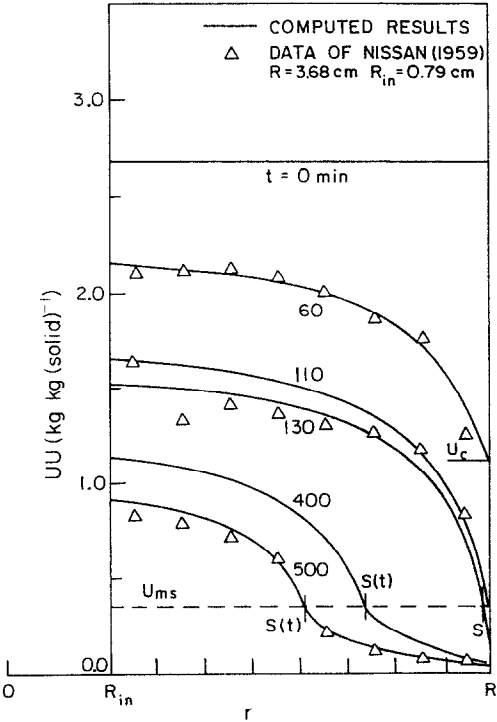


FIG. 5. Moisture distribution of wool during drying.

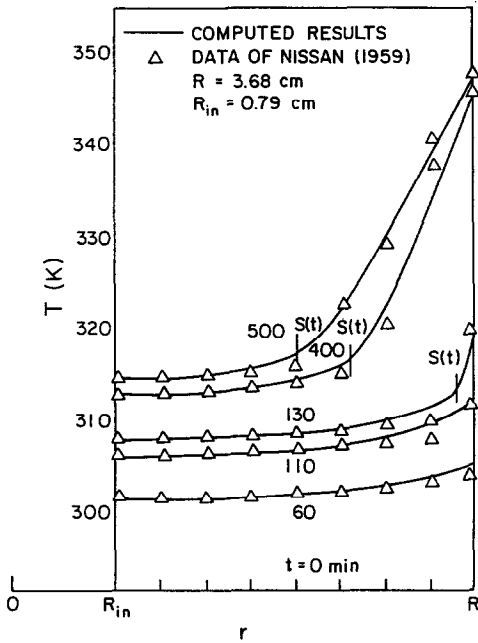


FIG. 6. Temperature distribution of wool during drying.

in Figs. 7–9. Figure 7 indicates the variation of the average moisture content with time; the predicted result shows a very short constant rate period (about 15 min). The second falling rate period starts at 78 min. The predicted temperature distribution at different times agrees well with the data, as shown in Fig. 8. No data on moisture distributions were reported.

Drying of corn kernels

The drying of individual or thin layers of corn kernels has been studied by many investigators [46–50]. In most of the experimental studies, the initial moisture content of the corn kernels is equal to or less than the maximum sorptive value. Thus, only the sorption region is involved and so no constant rate period will be observed. Therefore, movement of bound water and vapor flow are the main mechanisms

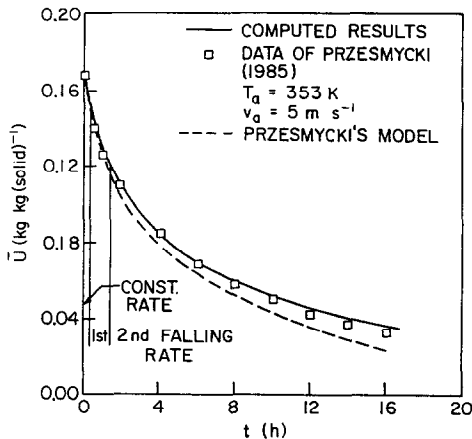


FIG. 7. Drying curve of brick.

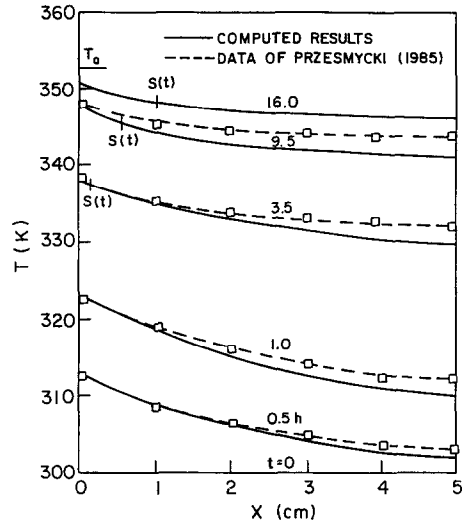


FIG. 8. Temperature distribution of brick during drying.

of internal moisture transfer. Furthermore, since the corn kernels are so small, they may be regarded as spherical.

The physical properties and the drying conditions are listed in Table 1 [48, 50, 51]; the sorption curve for yellow corn kernels was correlated from the data of Rodriguez-Arias [52]

$$\psi = \frac{P_v}{P_v^*} = 1 - \exp \left(- (0.43T - 75.0) U_2^{(3.18 - 0.0037T)} \right) \quad (44)$$

Considering only the sorption region, the numerical solutions for drying of individual or thin layers of corn kernels in two different air conditions were obtained, as shown in Figs. 10–12. The present model gives an excellent prediction of the drying curves reported in the literature [45, 47]. In grain drying processes, the problem of shrinkage often exists to

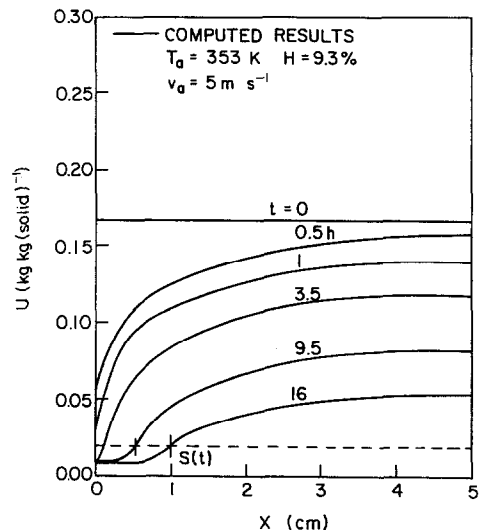


FIG. 9. Moisture distribution of brick during drying.

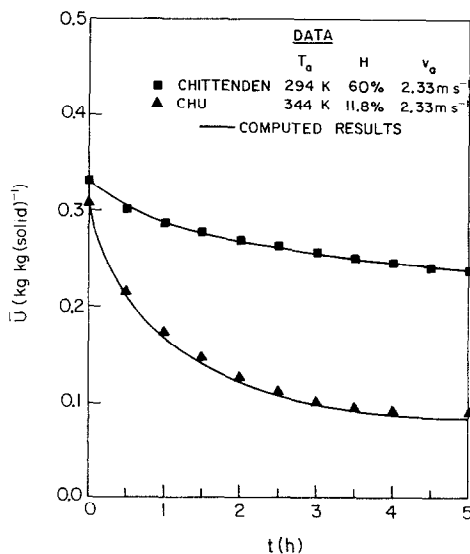


FIG. 10. Drying curve of corn kernels.

some extent. If the rate of shrinkage is known, the moving velocity of the outer surface can be taken into account. This can also be handled by the present drying model.

CONCLUSIONS

(1) A generalized mathematical model of drying processes is proposed. It has been successfully used to describe the drying behavior of several non-hygroscopic and hygroscopic materials. If the initial moisture content is high enough, a constant rate period will be observed. When the free water content at the surface reaches the critical, i.e. 30% of the saturated free water content, the continuous water layer at the surface breaks into wet patches and the first falling rate period starts. When the free water content at the surface is equal to zero, or the surface moisture content is equal to the maximum sorptive moisture

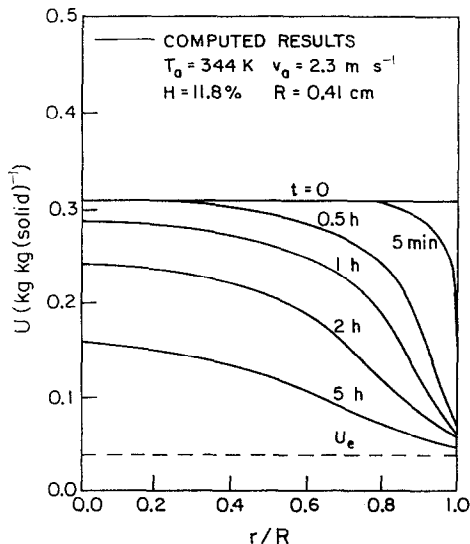


FIG. 11. Moisture distribution of corn kernels during drying.

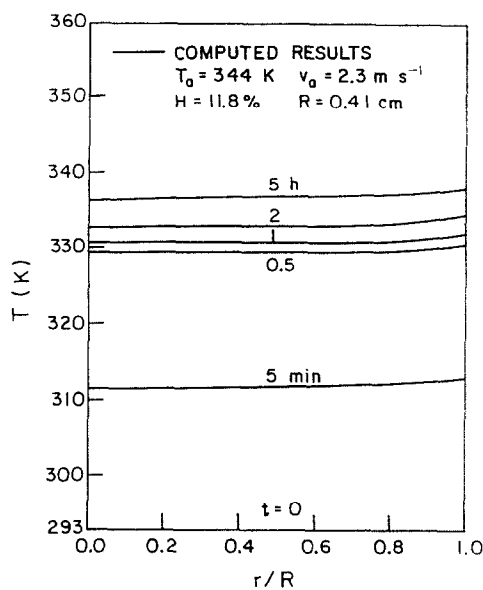


FIG. 12. Temperature distribution of corn kernels during drying.

content, the second falling rate period starts. During the second falling rate period, a receding evaporation front divides the material into wet and sorption regions, and the hygroscopic properties of the material will contribute to the drying rate.

(2) The mechanism of moisture transfer in the sorption region has been postulated as movement of bound water. In the sorption region, the local vapor pressure is related to the desorption isotherms, and therefore movement of bound water is also affected by the hygroscopic properties of the drying material. The bound water conductivity may be determined by equation (16).

(3) The convective heat and mass transfer coefficients vary with the free water content at the surface. Considering the effect of percolation threshold, a criterion of the free water content is defined, which has the value of about 30% of the saturated free water content. Thus, equations (22) and (23) may be used to estimate the varying heat and mass transfer coefficients during the first falling rate period.

(4) The present drying model has been successfully used to simulate the drying processes of brick, wool and corn kernels. The predicted drying curves and the temperature and moisture distributions compared favorably with the reported experimental results.

REFERENCES

- 1. M. Fortes and M. R. Okos, Drying theories; their bases and limitations as applied to food and grains. In *Advances in Drying* (Edited by A. S. Mujumdar), Vol. 1, pp. 119–154. Hemisphere, Washington, DC (1980).
- 2. J. L. Rossen and K. Hayakawa, Simultaneous heat and moisture transfer in dehydrated food: a review of theoretical models, *A.I.Ch.E. Symp. Ser.* 73, 71–81 (1977).
- 3. T. K. Sherwood, The drying of solids, *Ind. Engng Chem.* 21, 12–16 (1929).
- 4. T. K. Sherwood, Application of the theoretical diffusion

- equation to the drying of solids, *Trans. A.I.Ch.E.* **27**, 190–202 (1931).
5. N. H. Ceaglske and O. A. Hougen, Drying granular solids, *Ind. Engng Chem.* **29**, 805–813 (1937).
 6. C. J. King, *Freeze Drying of Foods*. Butterworth, London (1971).
 7. P. S. A. Henry, Diffusion in absorbing media, *Proc. R. Soc. London A* **171**, 215–241 (1939).
 8. T. Z. Harmathy, Simultaneous moisture and heat transfer in porous systems with particular reference to drying, *Ind. Engng Chem. Fund.* **8**, 92–103 (1969).
 9. R. A. Greenkorn, *Flow Phenomena in Porous Media*. Marcel Dekker, New York (1983).
 10. S. Whitaker, Flow in porous media II: the governing equations for immiscible, two-phase flow, *Transp. Porous Media* **1**, 105–125 (1986).
 11. O. Krischer and W. Kast, *Die Wissenschaftlichen Grundlagen der Trocknungstechnik*, 3rd Edn. Springer, Berlin (1978).
 12. D. Berger and D. C. T. Pei, Drying of hygroscopic capillary porous solids—a theoretical approach, *Int. J. Heat Mass Transfer* **16**, 293–302 (1973).
 13. A. V. Luikov, *Heat and Mass Transfer in Capillary-porous Bodies*. Pergamon Press, London (1966).
 14. A. V. Luikov, Systems of differential equations of heat and mass transfer in capillary-porous bodies, *Int. J. Heat Mass Transfer* **18**, 1–14 (1975).
 15. M. D. Mikhailov, Exact solution of temperature and moisture distribution in a porous half-space with moving evaporation front, *Int. J. Heat Mass Transfer* **18**, 797–804 (1975).
 16. S. Szentgyorgyi and K. Molnar, Calculation of drying parameters for the penetrating evaporating front, *Proc. 1st Int. Symp. on Drying* (Edited by A. S. Mujumdar), pp. 92–99. Science Press, Princeton, New Jersey (1978).
 17. P. Chen, Mathematical modelling of drying and freezing processes in the food industry, Ph.D. Thesis, University of Waterloo, Canada (1987).
 18. D. A. Rose, Water-movement in dry soils, physical factors affecting sorption of water by dry soil, *J. Soil Sci.* **19**, 81–93 (1968).
 19. E. Rotstein, Advances in transport phenomena and thermodynamics in the drying of cellular food systems. In *Drying'86* (Edited by A. S. Mujumdar), Vol. 1, pp. 1–11. Hemisphere, Washington, DC (1986).
 20. S. Whitaker, Moisture transport mechanisms during the drying of granular porous media. In *Drying'85* (Edited by A. S. Mujumdar), pp. 21–32. Hemisphere, Washington, DC (1985).
 21. M. Suzuki and S. Maeda, On the mechanism of drying of granular beds, mass transfer from discontinuous source, *J. Chem. Engng Japan* **1**, 26–31 (1968).
 22. J. Van Brakel and P. M. Heertjes, On the period of constant drying rate, *Proc. 1st Int. Symp. on Drying* (Edited by A. S. Mujumdar), pp. 70–75. Science Press, Princeton, New Jersey (1978).
 23. R. B. Kee, *Drying Principles and Practice*. Pergamon Press, Oxford (1972).
 24. E. Rotstein and A. R. H. Cornish, Influence of cellular membrane permeability on drying behavior, *J. Food Sci.* **43**, 926–934 (1978).
 25. R. G. Larson, L. E. Scriven and H. T. Davis, Percolation theory of two-phase flow in porous media, *Chem. Engng Sci.* **36**, 57–73 (1981).
 26. E. E. Miller and R. D. Miller, Theory of capillary flow I. Practical implications, *Proc. Soil Sci. Soc. Am.* **19**, 267–271 (1955).
 27. I. Chatzis, A network approach to analyse and model capillary and transport phenomena in porous media, Ph.D. Thesis, University of Waterloo, Canada (1980).
 28. G. Bramhall, Sorption diffusion in wood, *Wood Sci.* **12**, 3–13 (1979).
 29. S. Whitaker and W. T.-H. Chou, Drying granular porous media—theory and experiment, *Drying Tech. Int. J.* **1**, 3 (1983).
 30. J. Chirife, Fundamentals of the drying mechanism during air dehydration of foods. In *Advances in Drying* (Edited by A. S. Mujumdar), Vol. 2, pp. 73–102. Hemisphere, Washington, DC (1983).
 31. M. Okazaki, Heat and mass transport properties of heterogeneous materials. In *Drying'85* (Edited by R. Toei and A. S. Mujumdar), pp. 84–96. Hemisphere, Washington, DC (1985).
 32. H. Tamon, M. Okazaki and R. Toei, Flow mechanism of adsorbate through porous media in presence of capillary condensation, *A.I.Ch.E. J.* **27**, 271–277 (1981).
 33. C. K. Wei and H. T. Davis, Heat and mass transfer in water-laden sandstone: convective heating, *A.I.Ch.E. J.* **31**, 1338–1348 (1985).
 34. S. M. Henderson, Equilibrium moisture content of small grain hysteresis, *Trans. ASAE* **13**, 762–764 (1970).
 35. D. S. Chung and H. B. Post, Adsorption of water vapor by cereal grains and their products, *Trans. ASAE* **10**, 552–575 (1967).
 36. J. R. Bell and A. H. Nissan, Mechanism of drying thick porous bodies during the falling rate period, *A.I.Ch.E. J.* **5**, 344–347 (1959).
 37. A. H. Nissan, W. G. Kaye and J. R. Bell, Mechanism of drying thick porous bodies during the falling rate period, *A.I.Ch.E. J.* **5**, 103–110 (1959).
 38. S. O. Nelson, Moisture, frequency and density dependence of dielectric constant of shelled yellow-dent corn, *Trans. ASAE* **27**, 1573–1578 (1984).
 39. T. K. Ang, J. D. Ford and D. C. T. Pei, Microwave freeze-drying of food, a theoretical investigation, *Int. J. Heat Mass Transfer* **20**, 517–526 (1977).
 40. Y. H. Ma and P. Peltre, Mathematical simulation of freeze-drying, *A.I.Ch.E. J.* **21**, 335–344 (1975).
 41. D. R. Lynch and W. G. Gray, Finite element simulation of shallow water problem with moving boundaries. In *Finite Element Simulation in Water Resources*, Vol. 2. Pentech Press, London (1978).
 42. D. R. Lynch and K. O'Neil, Numerical solution of two phase Stefan problems using continuously deforming finite elements, *Int. J. Numer. Meth. Engng* **17**, 81–96 (1981).
 43. B. V. Walker, The drying characteristics of scoured wool, *N.Z. J. Sci.* **12**, 139–164 (1969).
 44. Z. Przesmycki and C. Strumillo, The mathematical modelling of drying process based on moisture transfer mechanism. In *Drying'85* (Edited by R. Toei and A. S. Mujumdar), pp. 126–134. Hemisphere, Washington, DC (1985).
 45. M. Haertling, Prediction of drying rates. In *Drying'80* (Edited by A. S. Mujumdar), Vol. 1, pp. 88–98. Hemisphere, Washington, DC (1980).
 46. D. H. Chittenden and A. Hustrulid, Determining drying constants for shelled-corn, *Trans. ASAE* **9**, 52–55 (1966).
 47. S. T. Chu and A. Hustrulid, General characteristics of variable diffusivity process and the dynamic equilibrium moisture content. *Trans. ASAE* **11**, 709–710 (1968).
 48. M. Fortes and M. R. Okos, Changes in physical properties of corn during drying, *Trans. ASAE* **23**, 1004–1008 (1980).
 49. H. Li and R. V. Morey, Thin-layer drying of yellow dent corn, *Trans. ASAE* **27**, 581–585 (1984).
 50. M. K. Misra and D. B. Brooker, Thin-layer drying and rewetting equations for shelled yellow corn, *Trans. ASAE* **23**, 1254–1260 (1980).
 51. S. M. Henderson and S. Pabis, Grain drying theory, I. Temperature effect on drying coefficient, *J. Agric. Engng Res.* **6**, 169–174 (1961).
 52. J. H. Rodriguez-Arias, Desorption isotherms and drying rates of shelled corn in the temperature range of 40–140°F, Ph.D. Thesis, Michigan State University, East Lansing, Michigan (1963).

UN MODELE MATHEMATIQUE DES MECANISMES DE SECHAGE

Résumé—On propose un modèle de séchage qui peut être utilisé pour décrire le séchage des matériaux hygroscopiques et non hygroscopiques. Les périodes de vitesse constante, de première diminution et de seconde diminution dans le séchage sont examinées séparément. On introduit le concept de "conductivité d'eau liée". On discute le mouvement de l'eau liée et sa contribution au transfert d'humidité dans les matériaux hygroscopiques. La conductivité de l'eau liée est affectée par le taux d'humidité et aussi par les isothermes de désorption du matériau. Les principaux mécanismes du transfert interne d'humidité sont considérés être l'écoulement capillaire de l'eau libre dans la région mouillée, le mouvement de l'eau liée et le transfert de vapeur dans la région de sorption. Les coefficients de convection de chaleur et de masse sont supposés variables avec le taux d'eau libre à la surface, dans la période de première diminution. Trois systèmes avec différentes propriétés hygroscopiques, bois, brique et grains de maïs, sont choisis pour évaluer la validité de ce modèle. La méthode des éléments finis mobiles est utilisée pour résoudre numériquement les équations différentielles. Les courbes de séchage et les profils de température et d'humidité calculés sont comparés favorablement aux résultats expérimentaux connus.

EIN MATHEMATISCHES MODELL FÜR TROCKNUNGSPROZESSE

Zusammenfassung—Es wird ein Modell vorgestellt, das zur Beschreibung des Trocknungsverhaltens von hygroscopischen und nicht-hygroscopischen Materialien herangezogen werden kann. Die einzelnen Trocknungsperioden werden getrennt betrachtet. Es wird das Konzept der "Leitfähigkeit des gebundenen Wassers" eingeführt. Die Bewegung des gebundenen Wassers und sein Beitrag zum Feuchtetransport innerhalb hygroscopischer Materialien wird diskutiert. Es wird herausgefunden, daß die Leitfähigkeit des gebundenen Wassers vom Feuchtegehalt sowie den Desorptionsisothermen des Trocknungsmaterials beeinflusst wird. Die wichtigsten internen Feuchtetransport-Mechanismen sind: die Kapillarströmung von freiem Wasser in der nassen Region und die Bewegung von gebundenem Wasser und Dampf in der Sorptionsregion. Es wird angenommen, daß sich der konvektive Wärme- und Stofftransport mit der freien Wasseroberfläche in der ersten Trocknungsperiode ändert. Für die Validierung des Modells werden drei Systeme mit unterschiedlichem hygroscopischem Verhalten—Wolle, Ziegel und Kornsamen—ausgewählt. Zur numerischen Lösung der Differentialgleichungen wird die Methode der beweglichen finiten Elemente herangezogen. Die berechneten Trocknungskurven und die Temperaturen und Feuchteverteilungen stimmen recht gut mit vorhandenen experimentellen Ergebnissen überein.

МАТЕМАТИЧЕСКАЯ МОДЕЛЬ ПРОЦЕССОВ СУШКИ

Аннотация—Предложена модель для описания сушки гигроскопичных и негигроскопичных материалов. Отдельно рассмотрены период постоянной скорости, первый и второй периоды падающей скорости сушки. Введено понятие теплопроводности связанной воды. Обсуждаются движение связанной воды и его вклад в перенос влаги в гигроскопичных материалах. Найдено, что на теплопроводность связанной воды влияют содержание влаги, а также изотермы десорбции высушиваемого материала. Считается, что основными механизмами переноса влаги являются капиллярное течение свободной воды во влажной области, а также движение связанной воды и перенос пара в области сорбции. Предполагается изменение коэффициентов конвективного тепло- и массопереноса с изменением содержания свободной воды на поверхности в первом периоде падающей скорости сушки. Для оценки пригодности данной модели выбраны три системы с различными гигроскопическими свойствами: шерсть, кирпич и кукурузное зерно. Дифференциальные уравнения решаются численно методом конечных элементов. Рассчитанные кривые сушки и распределения температуры и влаги удовлетворительно согласуются с экспериментальными данными.